

FLRW UNIVERSE IN $f(\mathcal{R}, \mathcal{L}_m)$ GRAVITY WITH EQUATION OF STATE PARAMETER

✉ **Bhupendra Kumar Shukla**^a, ✉ **R.K. Tiwari**^b, ✉ **D. Sofuoğlu**^c, ✉ **A. Beesham**^{d,e,f*}

^a Department of Mathematics, Govt. College Bandri Sagar 470442 (M.P.) India

^b Department of Mathematics, Govt. Model Science College Rewa 486 001 (M.P.) India

^c Department of Physics, Istanbul University Vezneciler 34134, Fatih, Istanbul, Turkey

^d Department of Mathematical Sciences, University of Zululand, P Bag X1001, Kwa-Dlangezwa 3886, South Africa

^e Faculty of Natural Sciences, Mangosuthu University of Technology, P O Box 12363, Jacobs, South Africa

^f National Institute for Theoretical and Computational Sciences, South Africa

* Corresponding Author e-mail: abeesham@yahoo.com

Received October 16, 2023; revised November 19, 2023; accepted November 22, 2023

Available observational data regarding current cosmological characteristics suggest that the universe is, to a large extent, both isotropic and homogeneous on a large scale. In this study, our objective is to analyze the Friedmann-Lemaitre-Robertson-Walker (FLRW) space time using an perfect fluid distribution. We specifically investigate the framework of $f(\mathcal{R}, \mathcal{L}_m)$ gravity within certain constraints. To accomplish this, we concentrate on a specific nonlinear $f(\mathcal{R}, \mathcal{L}_m)$ model, represented by $f(\mathcal{R}, \mathcal{L}_m) = \frac{\mathcal{R}}{2} + \mathcal{L}_m^\alpha$. The field equations are solved using the equation of state parameter of the form of the Chevallier-Polarski-Linder (CPL) parameterization. The deceleration parameter study finds an accelerating universe at late times. The transition redshift is found to be $z_{tr} = 0.89 \pm 0.25$. Also we discuss the physical and geometrical properties of the model.

Keywords: $f(\mathcal{R}, \mathcal{L}_m)$ gravity; Dark energy; Acceleration of universe; Equation of state parameter

PACS: 98.80.-k

1. INTRODUCTION

Recent astronomical observations have compellingly substantiated the ongoing expansion of the universe. The concept of cosmic acceleration garners support from diverse sources, encompassing high-redshift supernovae, the cosmic microwave background radiation (CMBR), data derived from the Wilkinson Microwave Anisotropy Probe (WMAP), baryonic acoustic oscillations (BAOs), and the intricate large-scale structure (LSS) [1, 2, 3, 4, 5, 6, 7, 8, 9] of the cosmos. These observations have disclosed the presence of an enigmatic entity known as Dark Energy (DE), which permeates the universe and accounts for approximately 70% of its aggregate energy content. Dark Energy possesses an intriguing trait: it exerts a potent negative pressure, setting it apart from conventional manifestations of matter and energy. This enigmatic quality enhances both the complexity and allure of our pursuit to comprehend the fundamental mechanisms governing the universe. Dark Energy assumes a pivotal role in propelling the accelerated expansion of the universe and is quantified by its equation of state (EoS) parameter, symbolized as $\omega = \frac{p}{\rho}$, where p denotes pressure, and ρ signifies energy density. A multitude of investigations have demonstrated that when the EoS parameter approaches $\omega = -1$ [10, 11], the universe undergoes accelerated expansion. Under specific conditions, Dark Energy can manifest phantom-like behavior, indicated by $\omega < -1$. In such scenarios, a universe governed by phantom Dark Energy is predicted to confront an impending singularity referred to as cosmic doomsday or the big rip, a cataclysmic event where the very fabric of the universe is torn asunder [12, 13, 14]. To illuminate and elucidate the intrinsic nature of Dark Energy and its association with late-time acceleration, scientists have immersed themselves in the exploration of modified theories of gravity. These alternative theories provide an intriguing avenue distinct from conventional approaches, holding the potential to unveil the enigmatic aspects surrounding cosmic acceleration and quintessence [15].

A recent development in the field of gravitational theories comes from Harko et al. [16], who have introduced a novel generalization known as the $f(\mathcal{R}, \mathcal{L}_m)$ theory of gravity. In this theory, ' \mathcal{R} ' represents the scalar curvature, and ' \mathcal{L}_m ' corresponds to the matter Lagrangian density. This extension presents a fresh perspective on understanding gravitational dynamics by simultaneously incorporating the geometric property of curvature and the energy distribution described by the matter Lagrangian density. This intriguing interconnection between matter and geometry results in an additional force that acts perpendicular to the four-velocity vector, leading to the non-geodesic motion of massive particles. Expanding on this concept, researchers have extended

their investigations to explore arbitrary couplings in both matter and geometry [17]. They have conducted comprehensive inquiries into the cosmological and astrophysical implications arising from these non-minimal matter-geometry couplings [18, 19, 20, 21, 22]. It is worth noting that $f(\mathcal{R}, \mathcal{L}_m)$ gravity models explicitly violate the equivalence principle, which has been rigorously constrained by tests within the solar system [23, 24].

Recently, Wang and Liao conducted a study examining energy conditions within the framework of $f(\mathcal{R}, \mathcal{L}_m)$ gravity [25]. Additionally, Goncalves and Moraes analyzed cosmological aspects by considering the non-minimal matter-geometry coupling in $f(\mathcal{R}, \mathcal{L}_m)$ gravity [26]. Solanki et al. made a significant contribution to the background of $f(\mathcal{R}, \mathcal{L}_m)$ by investigating cosmic acceleration within an anisotropic space-time with bulk viscosity [27]. Furthermore, Jaybhaye et al. carried out an insightful study focusing on constraining the equation of state for viscous Dark Energy in the context of $f(\mathcal{R}, \mathcal{L}_m)$ gravity [28]. Their research provides valuable insights into our understanding of the nature of Dark Energy within this specific gravitational framework, thereby contributing to our broader comprehension of cosmic acceleration and its underlying mechanisms. These studies shed light on the intriguing consequences of the interaction between matter and geometry in the context of $f(\mathcal{R}, \mathcal{L}_m)$ gravity. Presently, there is a growing body of literature exploring the fascinating cosmological implications of the $f(\mathcal{R}, \mathcal{L}_m)$ gravity theory [29, 30, 31, 32, 33, 34, 35, 36, 37]. Numerous studies have emerged, delving into various aspects and implications of this theory [38, 39, 40, 41].

In this work, we select the function $f(\mathcal{R}, \mathcal{L}_m)$ to be given by:

$$f(\mathcal{R}, \mathcal{L}_m) = \frac{R}{2} + \mathcal{L}_m^\alpha \tag{1}$$

where R denotes the Ricci scalar and \mathcal{L}_m denotes the matter Lagrangian. If $\alpha = 0$, then, as pointed out by Harko and Lobo [16], we recover the Hilbert-Einstein Lagrangian and the field equations of general relativity. Now the most general function for $f(\mathcal{R}, \mathcal{L}_m)$ gravity is given by Harko and Lobo [43]:

$$f(\mathcal{R}, \mathcal{L}_m) = \frac{1}{2}f_1(R) + G(\mathcal{L}_m)f_2(R) \tag{2}$$

where $f_1(R)$ and $f_2(R)$ are arbitrary, but analytical, functions of the Ricci scalar R and $G(\mathcal{L}_m)$ is an arbitrary, but analytical, function of the matter Lagrangian density \mathcal{L}_m . Since we are interested in a simple deviation from general relativity, we choose the function $f(\mathcal{R}, \mathcal{L}_m)$ to be given by (1). In addition, choosing the function $f_1(R)$ to be arbitrary essentially yields $f(R)$ gravity, and this has been extensively studied in the literature [43]. So we concentrate on the function $G(\mathcal{L}_m)$, and again, for simplicity, we choose $f_2(R) = 1$ and $G(\mathcal{L}_m) = \mathcal{L}_m^\alpha$. These choices are sufficient to enable the equations to be tractable, as well as to indicate broadly the differences from general relativity.

Most studies involving Dark Energy in modified theories have to make some assumption on one of the parameters such as the scale factor, Hubble parameter, deceleration parameter or equation of state (EoS). In this work, we assume a form for the EoS. Our work is arranged as follows. In section II, we give a brief review of $f(\mathcal{R}, \mathcal{L}_m)$ gravity. Our model is discussed in section III. Observational constraints are imposed on the model in section IV. Section V entails the cosmographic parameters. We discuss the physical parameters in section VI. Section VII provides a discussion on the energy conditions. Finally, we conclude in section VIII.

2. REVIEW OF $f(\mathcal{R}, \mathcal{L}_m)$ GRAVITY

The gravitational action for $f(R, \mathcal{L}_m)$ is given by

$$S = \int f(R, \mathcal{L}_m)\sqrt{-g}dx^4. \tag{3}$$

Here R denotes the Ricci scalar and \mathcal{L}_m denotes the matter Lagrangian. The Ricci scalar R is obtained by contracting the Ricci tensor $R_{\mu\nu}$ as

$$R = g^{\mu\nu} R_{\mu\nu}, \tag{4}$$

where the Ricci tensor $R_{\mu\nu}$ can also be written in the following form:

$$R_{\mu\nu} = \partial_\lambda \Gamma_{\mu\nu}^\lambda - \partial_\mu \Gamma_{\lambda\nu}^\lambda + \Gamma_{\mu\nu}^\lambda \Gamma_{\sigma\lambda}^\sigma - \Gamma_{\nu\sigma}^\lambda \Gamma_{\mu\lambda}^\sigma, \tag{5}$$

with $\Gamma_{\alpha\beta}^\lambda$ representing the components of Levi-Civita connection.

Now the given field equations are obtained by variation with respect to the metric tensor $g_{\mu\nu}$:

$$f_R R_{\mu\nu} + (g_{\mu\nu}\square - \nabla_\mu \nabla_\nu)f_R - \frac{1}{2}(f - f_{\mathcal{L}_m} \mathcal{L}_m)g_{\mu\nu} = \frac{1}{2}f_{\mathcal{L}_m} T_{\mu\nu}, \tag{6}$$

Here $f_R = \frac{\partial f}{\partial R}$, $f_{\mathcal{L}_m} = \frac{\partial f}{\partial \mathcal{L}_m}$ and $T_{\mu\nu}$, the stress-energy tensor for the cosmic fluid, is given by:

$$T_{\mu\nu} = \frac{-2}{\sqrt{-g}} \frac{\delta(\sqrt{-g}\mathcal{L}_m)}{\delta g^{\mu\nu}}. \tag{7}$$

Now, we can obtain the following relation by using the covariant derivative in equation (6)

$$\nabla^\mu T_{\mu\nu} = 2\nabla^\mu \ln(f_{\mathcal{L}_m}) \frac{\partial \mathcal{L}_m}{\partial g^{\mu\nu}}. \tag{8}$$

The homogeneous and spatially isotropic FLRW metric is given by:

$$ds^2 = -dt^2 + a^2(t)(dx^2 + dy^2 + dz^2), \tag{9}$$

where $a(t)$ is the cosmic scale factor. Now, the Ricci scalar for the metric (9) is obtained as:

$$R = 6(\dot{H} + 2H^2), \tag{10}$$

where H is the Hubble parameter given by:

$$H = \frac{\dot{a}}{a}. \tag{11}$$

For a perfect fluid

$$T_{\mu\nu} = (\rho + p)u_\mu u_\nu + pg_{\mu\nu}. \tag{12}$$

where ρ is the energy density and p the pressure, the corresponding field equations are given by:

$$3H^2 f_R + \frac{1}{2}(f - f_R R - f_{\mathcal{L}_m} \mathcal{L}_m) + 3H \dot{f}_R = \frac{1}{2} f_{\mathcal{L}_m} \rho, \tag{13}$$

$$\dot{H} f_R + 3H^2 f_R - \ddot{f}_R - 3H \dot{f}_R + \frac{1}{2}(f_{\mathcal{L}_m} \mathcal{L}_m - f) = \frac{1}{2} f_{\mathcal{L}_m} p. \tag{14}$$

3. $f(\mathcal{R}, \mathcal{L}_m)$ GRAVITY MODEL

Since $f(\mathcal{R}, \mathcal{L}_m)$ is an arbitrary function of R and L_m , we choose $f(\mathcal{R}, \mathcal{L}_m)$ as:

$$f(\mathcal{R}, \mathcal{L}_m) = \frac{R}{2} + \mathcal{L}_m^\alpha, \tag{15}$$

where n is free parameter. Following this, for that particular functional type of $\mathcal{L}_m = \rho$ [42], the universe is given by the Friedmann equations (13) and (14):

$$3H^2 = (2\alpha - 1)\rho^\alpha, \tag{16}$$

$$2\dot{H} + 3H^2 = [(\alpha - 1)\rho - \alpha p]\rho^{\alpha-1}. \tag{17}$$

In cosmology, the effective equation of state parameter, often denoted as ω_{eff} is a quantity used to describe the behavior of the dark energy component of the universe. Dark energy is a mysterious form of energy that is thought to be responsible for the observed accelerated expansion of the universe. The equation of state parameter for dark energy, ω , relates the pressure (p) and energy density (ρ) of dark energy through the equation:

$$\omega = \frac{p}{\rho} \tag{18}$$

Now using equations (16) and (17) we get:

$$\omega = -1 + \frac{(2 - 4\alpha)\dot{H}}{3\alpha H^2} \tag{19}$$

3.1. Observational Evidence and Precision Cosmology (Late 20th Century - Present)

Over the years, various cosmological observations, such as the study of Type Ia supernovae, the cosmic microwave background, and large-scale structure, have been used to constrain the value of ω . Current observations suggest that the equation of state parameter for dark energy is close to $\omega = -1$, consistent with a cosmological constant (Λ). However, the possibility of a time-varying equation of state parameter (dynamic dark energy models) has also been explored to explain the observed cosmic acceleration. In summary, the historical discussion of the equation of state parameter in cosmology evolved from its early introduction by Einstein to maintain a static universe, to its modern interpretation as a way to describe the properties of dark energy, which plays a crucial role in the accelerated expansion of the universe.

Observational evidence and precision cosmology have helped refine our understanding of ω and its implications for the nature of dark energy. In the exploration of Dark Energy (DE), researchers have introduced various parameterizations of the Equation of State (EoS) parameter to capture its dynamic characteristics. One commonly employed parameterization is the Chevallier-Polarski-Linder (CPL) parameterization:

$$\omega(z) = n + \frac{mz}{(1+z)}, \quad (20)$$

which is derived from a straightforward Taylor expansion of the EoS with respect to the scale factor [43, 44]. While the CPL parameterization is a dependable choice for characterizing the behavior of the Universe during early ($z \rightarrow \infty$) and present ($z = 0$) epochs, it exhibits singular behavior at future times. Precisely, it encounters issues at a redshift of $z = -1$. Nevertheless, it is worth noting that the CPL parameterization performs effectively at high redshifts and serves as a suitable approximation for slow-roll DE scalar field models. From equations (17) and (18), we obtain:

$$H = \left[(1+z)^{1+m+n} \exp\left(\frac{m}{1+z}\right) \right]^{\frac{3\alpha}{(4\alpha-2)}} \quad (21)$$

4. OBSERVATIONAL CONSTRAINTS

Observational constraints on cosmological models are crucial for understanding the nature and evolution of our universe. One of the fundamental observations used for this purpose is the Hubble parameter ($H(z)$) data, which provides valuable information about the expansion rate of the universe as a function of redshift (z). In this discussion, we will delve into the use of Hubble Data as an observational constraint in cosmology.

Hubble Parameter ($H(z)$): The Hubble parameter is a measure of the rate at which the universe is expanding at a given cosmic time. It is a fundamental parameter in cosmology and is related to the Hubble constant (H_0), which represents the current expansion rate of the universe. In a homogeneous and isotropic universe, the Hubble parameter can be expressed as:

$$H(z) = H_0 \cdot E(z), \quad (22)$$

where $E(z)$ is known as the dimensionless Hubble parameter and is defined as:

$$E(z) = \sqrt{\Omega_m(1+z)^3 + \Omega_\Lambda}, \quad (23)$$

Here, Ω_m , and Ω_Λ represent the densities of matter, radiation, and dark energy, respectively.

Using Hubble Data for Observational Constraints:

Data Collection: Observational constraints on $H(z)$ typically involve collecting data from various astronomical observations. These observations can include measurements of the Hubble parameter at different redshifts, often obtained through techniques like supernova observations, baryon acoustic oscillations (BAO), or cosmic microwave background (CMB) experiments.

Model-Dependent and Model-Independent Approaches:

Model-Dependent: In this approach, cosmologists assume a particular cosmological model, which may include parameters like Ω_m , Ω_Λ , and others. The model's predicted $H(z)$ is then compared to the observed data. Adjusting the model parameters helps find the best-fit values that match the observations.

Model-Independent: Alternatively, cosmologists can analyze the data in a model-independent way. In this case, they use parametric or non-parametric methods to reconstruct $H(z)$ without making strong assumptions about the underlying cosmological model. This approach is valuable for testing the concordance model (Λ CDM) and identifying deviations from it.

Chi-Square Test: To quantify the agreement between the theoretical predictions and observed $H(z)$ measurements, cosmologists often employ a statistical tool known as the chi-square (χ^2) test. The χ^2 test calculates a statistic that quantifies the goodness of fit between the model and the data. Smaller values of χ^2 indicate a better match between the model and observations.

$$\chi^2 = \sum_i \frac{(H_{\text{obs},i} - H_{\text{th},i})^2}{\sigma_i^2}, \tag{24}$$

$H_{\text{obs},i}$: Observed Hubble parameter at redshift z_i . $H_{\text{th},i}$: Theoretical prediction for the Hubble parameter at redshift z_i based on the model. σ_i : Uncertainty (error) associated with the observed $H(z)$ at redshift z_i .
Parameter Estimation: In the model-dependent approach, the χ^2 test helps constrain the values of cosmological parameters, such as the matter density (Ω_m) or dark energy density (Ω_Λ). The goal is to find parameter values that minimize χ^2 , indicating the best agreement between the model and the data.

Model Testing: Observational constraints on $H(z)$ are used to test the validity of different cosmological models, including extensions to the standard Λ CDM model. Deviations between the observed data and model predictions can provide insights into the nature of dark energy, the expansion history of the universe, and potential departures from the standard model.

Cosmic Chronometers: The measurement of $H(z)$ is often referred to as "cosmic chronometry." This approach allows cosmologists to track the cosmic expansion history and assess the behavior of dark energy over cosmic time.

In summary, observational constraints using the Hubble Data in cosmology involves collecting measurements of the Hubble parameter at various redshifts and comparing them to theoretical predictions. These constraints help determine the properties of the universe, the nature of dark energy, and the validity of cosmological models, ultimately advancing our understanding of the cosmos. The chi-square test is a powerful tool for quantifying the agreement between observations and models, allowing cosmologists to extract valuable information about the evolution of the universe.

The priors that we used for the calculation of the model parameters α , m and n are obtained as follows. From equations (16) and (17), we see that $\alpha = 1$ corresponds to general relativity, so we choose (0, 2) as the prior for α . From the equation (20) for $w(z)$, we see that as $z \rightarrow 0$, $\omega(0) = n$. Since $\omega(0) = -1$ for the Λ CDM model, and we do not want a large departure from the Λ CDM model, we take $(-2, 0)$ as the prior for n . For m , we observe that for large z , i.e., at early times, the universe is decelerating, or $\omega(z) \equiv p/\rho > 0$. Now, from equation (20), for $z \rightarrow \infty$, $\omega = n + m$. From the fact that $\omega(z) > 0$ at early times and bounds on the prior for n , we choose (2, 4), as the prior for m .

We now summarise our results for our parameters H_0 , α , m and n using the above-mentioned tests:

| MCMC Results | | | | |
|--------------|-----------|-------------------------|------------------|---------------------|
| Dataset | Parameter | $f(R, L_m)$ Model | Parameter | Λ CDM Model |
| CC | H_0 | 69 ± 0.012 | H_0 | 67.4 |
| | α | $1.58^{+0.29}_{-0.35}$ | Ω_m | 0.325231 |
| | m | $4.03^{+0.29}_{-0.59}$ | Ω_Λ | 0.857423 |
| | n | $-1.71^{+0.11}_{-0.11}$ | | |

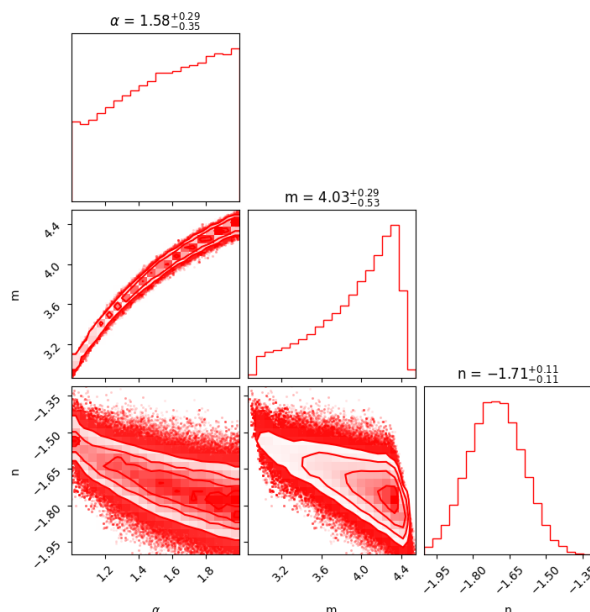


Figure 1. This graph shows the MCMC confidence contours at the 1σ and 2σ levels obtained from the 31 CC datasets.

In Fig. 1, we have plotted the likelihood contours for model parameters H_0, α, m and n at the 1σ and 2σ levels obtained from the 31 Cosmic Chronometers (CC) dataset. The CC dataset comprises the 31 data points, obtained from the differential age method, spanning the redshift range $0.07 < z < 2.42$. The best-fit values for the model parameters obtained are $H_0 = 69 \pm 0.012$, $\alpha = 1.58^{+0.29}_{-0.35}$, $m = 4.03^{+0.29}_{-0.59}$, and $n = -1.71^{+0.11}_{-0.11}$.

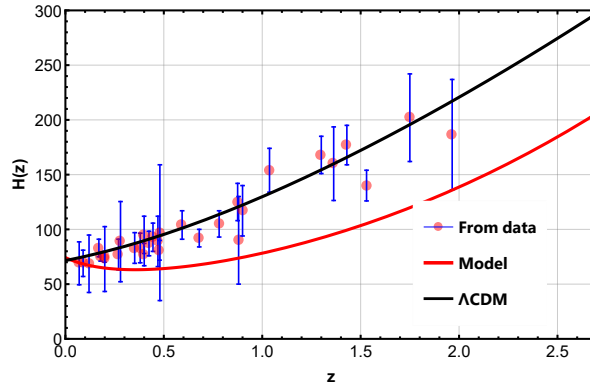


Figure 2. This figure shows our $H(z)$ curve compared to that of the Λ CDM model.

In Fig. 2, we have plotted the curves of $H(z)$ for both the Λ CDM and our models. To plot the curve for our model, we made use of the $H(z)$ equation given by (21), and values of the model parameters $\alpha = 1.58, m = 4.03$ and $n = -1.71$ from our Table.

5. COSMOGRAPHIC PARAMETERS

Cosmographic parameters constitute a collection of cosmological quantities employed to depict the historical expansion of the universe. These parameters are typically derived through a series expansion of scale factor of the universe as a function of cosmic time. This cosmographic approach offers a model-independent means of investigating the expansion of the universe, free from reliance on particular models related to dark energy or dark matter. Among the commonly utilized cosmographic parameters are the Hubble parameter (H), the deceleration parameter (q), the jerk parameter (j), and higher-order parameters. These parameters provide valuable insights into the behavior of the universe at different cosmic epochs and play a role in assessing various cosmological models.

5.1. Deceleration Parameter (q):

The deceleration parameter, denoted as q , stands as a pivotal cosmographic parameter characterizing whether the expansion of the universe is slowing down or accelerating. It is defined as the negative of the ratio between cosmic acceleration and cosmic expansion rate, expressed as:

$$q = -\frac{\ddot{a}}{aH^2}, \tag{25}$$

Here, a represents the scale factor of the universe, H denotes the Hubble parameter, and \ddot{a} signifies the second derivative of the scale factor with respect to cosmic time.

We obtain the deceleration parameter in terms of redshift as:

$$q(z) = -1 + \frac{3\alpha \left((1+m+n) - \frac{n}{1+z} \right)}{(4\alpha - 2) \left[(1+z)^{(1+m+n)} \text{Exp} \left(\frac{n}{1+z} \right) \right]^{\frac{4-\alpha}{4\alpha-2}}}. \tag{26}$$

The deceleration parameter yields essential insights into cosmic dynamics: When $q > 0$, it signifies deceleration, indicating that matter and gravity predominantly influence cosmic expansion. Conversely, when $q < 0$, it suggests acceleration, a hallmark feature of dark energy. In cases involving a cosmological constant (Λ) or forms of dark energy characterized by negative pressure, q is expected to be less than zero.

We now show how we calculate the value of the transition redshift $z_{tr} = 0.89 \pm 0.25$ as in the abstract. The transition redshift is the redshift at which the universe transits from deceleration to acceleration, and is given by $q = 0$. In the table at the end of section 4, we have illustrated the best-fit values of the parameters α, m and n from the chi-squared test using observational values of the Hubble parameter. We substitute these values into equation (26) and put $z = 0$. This give us the value of the transition redshift as $z_{tr} = 0.89 \pm 0.25$. By using the values $\alpha = 1.58, m = 4.03$ and $n = -1.71$ from our table in equation (26), we have illustrated $q(z)$ in Fig. 3.

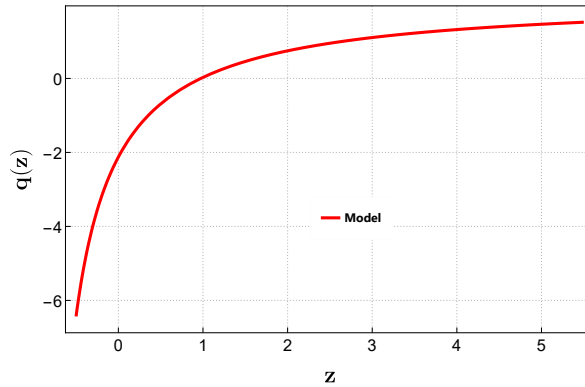


Figure 3. This figure illustrates the deceleration parameter $q(z)$.

It should be pointed out that values of the parameters different from our calculated ones of $\alpha = 1.58$, $m = 4.03$ and $n = -1.71$ can lead to undesirable consequences, such as no transition from deceleration to acceleration and values of the transition redshift that are inconsistent with observations. Similarly, a “bad” choice of the function $f(\mathcal{R}, \mathcal{L}_m)$ can also lead to these problems.

5.2. Statefinder Parameters:

The statefinder parameters encompass a collection of dimensionless cosmological parameters introduced to explore the expansion dynamics of the universe in a model-independent manner. They are derived from derivatives of the scale factor concerning cosmic time and are valuable for distinguishing between different cosmological models and detecting deviations from the conventional Λ CDM model.

Two of the significant statefinder parameters are r and s defined as:

$$r = \frac{\ddot{a}}{aH^3}, \tag{27}$$

$$s = \frac{r - 1}{3(q - 1/2)}, \tag{28}$$

These parameters depend on the scale factor (a), Hubble parameter (H), the third derivative of the scale factor with respect to cosmic time (\ddot{a}), and the deceleration parameter (q).

We now wish to write the statefinder parameters (r, s) from equations (27) and (28) in terms of $H(z)$, its derivatives and $q(z)$:

$$r(1+z) = 1 - 2\frac{H'}{H}(1+z) + \left[\frac{H''}{H} + \left(\frac{H'}{H}\right)^2 \right] (1+z)^2 \tag{29}$$

$$s(1+z) = \frac{r(1+z) + 1}{3[q(1+z) - 1/2]} \tag{30}$$

where the primes denote derivatives with respect to $(1+z)$. To write r and s in terms of z , we use equations (21), and its derivatives, and (26), thereby obtaining equations (29) and (30). These are plotted in Fig. 4 and Fig. 5.

Statefinder parameters are particularly useful in discerning various dark energy models. In the context of the Λ CDM model, both r and s assume fixed values ($r = 1$ and $s = 0$). Deviations from these values can indicate the presence of alternative dark energy models or theories of modified gravity.

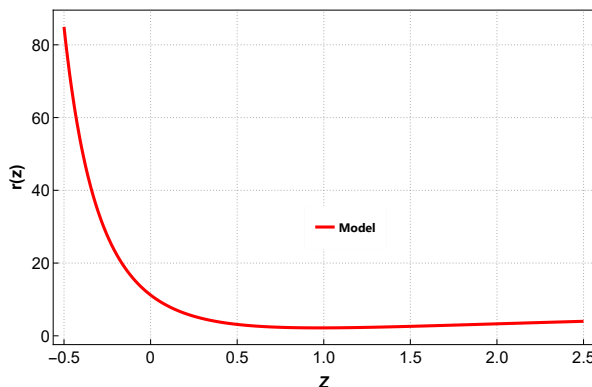


Figure 4. This figure shows the parameter $r(z)$.

Fig. 4 shows the curve $r(z)$. This is obtained from equations (29), (21), (26) and the parameter values $\alpha = 1.58, m = 4.03$ and $n = -1.71$ from our table.

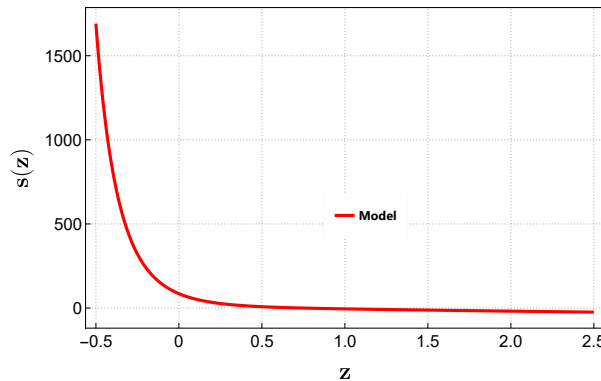


Figure 5. This figure shows the parameter $s(z)$.

Fig. 5 shows the curve $s(z)$. This is obtained from equations (30), (29) and (26), and the parameter values $\alpha = 1.58, m = 4.03$ and $n = -1.71$ from our table.

In summary, cosmographic parameters, including the deceleration parameter (q) and statefinder parameters (r and s), provide valuable insights into the dynamics of cosmic expansion. They enable cosmologists to investigate the effects of dark energy and modified gravity theories without committing to specific models, contributing significantly to our comprehension of the evolution of the cosmos.

6. PHYSICAL PARAMETERS

In cosmology, the behavior of the energy density and pressure plays a crucial role in determining the evolution and dynamics of the universe. These two quantities are described by the energy-momentum tensor and are governed by the equations of state for different components of the cosmic content, such as matter, radiation, and dark energy. Here, we will briefly discuss the behavior of the energy density and pressure in our model:

$$\rho = \left[\frac{3 \left[(1+z)^{1+m+n} \exp\left(\frac{m}{1+z}\right) \right]^{\frac{6\alpha}{(4\alpha-2)}}}{(2\alpha-1)} \right]^{\frac{1}{\alpha}}, \tag{31}$$

$$p = - \frac{\frac{3\alpha}{(2\alpha-1)} \left[(1+z)^{1+m+n} \exp\left(\frac{m}{1+z}\right) \right]^{\frac{6\alpha}{(4\alpha-2)}}}{\alpha \left[\frac{3 \left[(1+z)^{1+m+n} \exp\left(\frac{m}{1+z}\right) \right]^{\frac{6\alpha}{(4\alpha-2)}}}{(2\alpha-1)} \right]^{\frac{\alpha-1}{\alpha}}} + \frac{\left[(1+z)^{1+m+n} \exp\left(\frac{m}{1+z}\right) \right]^{\frac{6\alpha}{(4\alpha-2)}} \left[\frac{3\alpha \left((1+m+n) - \frac{n}{1+z} \right)}{(4\alpha-2) \left[(1+z)^{(1+m+n)} \exp\left(\frac{n}{1+z}\right) \right]^{\frac{4-\alpha}{4\alpha-2}}} \right]}{\alpha \left[\frac{3 \left[(1+z)^{1+m+n} \exp\left(\frac{m}{1+z}\right) \right]^{\frac{6\alpha}{(4\alpha-2)}}}{(2\alpha-1)} \right]^{\frac{\alpha-1}{\alpha}}}. \tag{32}$$

6.1. Matter-Dominated Universe:

Energy Density (ρ): In a matter-dominated universe, such as the present cosmic era, the energy density associated with matter (both dark matter and baryonic matter) dominates. In general relativity, the energy density of matter scales with the volume of the universe, decreasing as the universe expands. Specifically, for non-relativistic matter (where particles move much slower than the speed of light), the energy density scales as $\rho \propto a^{-3}$, where a is the scale factor of the universe.

Pressure (p): In the case of non-relativistic matter, the pressure is negligible ($p \approx 0$). Ordinary matter particles do not exert significant pressure on the universe’s expansion. Therefore, matter contributes to cosmic deceleration due to its gravitational attraction.

6.2. Radiation-Dominated Universe:

Energy Density (ρ): In the early universe, during radiation domination (e.g., during the era of the cosmic microwave background radiation), radiation (including photons and relativistic particles) dominates the energy density. Radiation energy density scales differently from matter and decreases faster with cosmic expansion: In general relativity, $\rho \propto a^{-4}$. This rapid decrease is due to the redshifting of photon energies as the universe expands.

Pressure (p): Radiation exerts significant pressure (In general relativity, $p = \frac{1}{3}\rho$). The high pressure associated with radiation contributes to the early rapid expansion of the universe. It leads to the deceleration of cosmic expansion, but at a slower rate compared to the matter-dominated era.

6.3. Dark Energy-Dominated Universe:

Energy Density (ρ): In the current era, observations suggest that dark energy dominates the energy density of the universe. Unlike matter and radiation, dark energy does not dilute with cosmic expansion (its energy density remains nearly constant).

Pressure (p): Dark energy is characterized by negative pressure ($p < 0$), and it behaves like a cosmological constant (Λ) in the Λ CDM model. This negative pressure drives cosmic acceleration, causing the universe to expand at an accelerating rate. The pressure of dark energy counteracts the gravitational attraction of matter and radiation, leading to the observed cosmic acceleration.

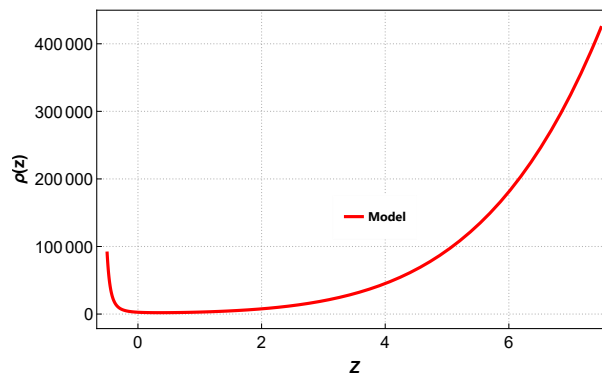


Figure 6. This figure illustrates the energy density $\rho(z)$.

In Fig. 6 we have plotted the energy density $\rho(z)$ from equation (31), using the parameter values $\alpha = 1.58, m = 4.03$ and $n = -1.71$ from our table. We notice that the energy density is non-negative.

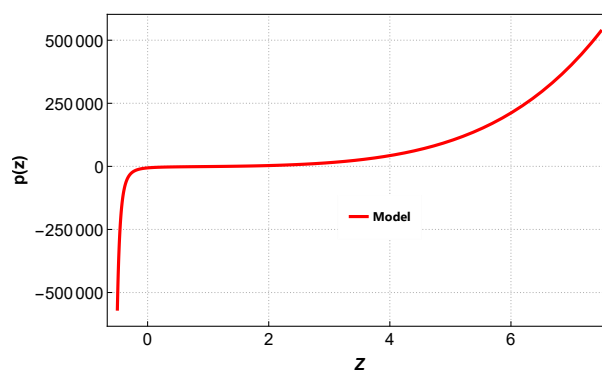


Figure 7. This figure illustrates the pressure $p(z)$.

In Fig. 7 we have plotted the pressure $p(z)$ from equation (32), using the parameter values $\alpha = 1.58, m = 4.03$ and $n = -1.71$ from our table. The Fig shows that the pressure is initially positive (deceleration), but at a redshift of $z_{tr} = 0.89 \pm 0.25$, it changes sign from positive to negative, signifying a transition from deceleration to acceleration.

6.4. Equation of State:

The relationship between energy density and pressure is often described by an equation of state parameter ($w \equiv p/\rho$). For matter, $w \approx 0$, for radiation, $w = \frac{1}{3}$, and for dark energy in the Λ CDM model, $w = -1$. Different components with varying values of w have distinct effects on cosmic expansion and evolution.

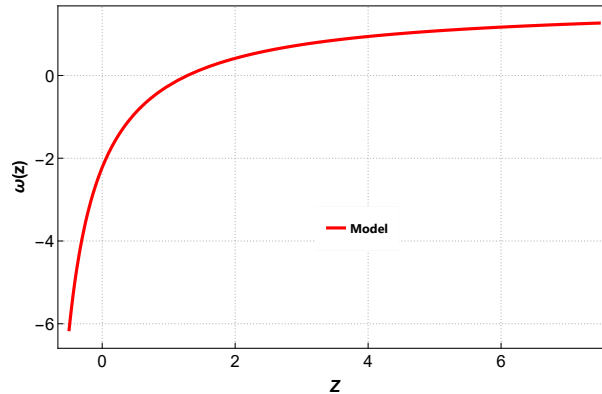


Figure 8. This figure shows the EoS $\omega(z)$.

In Fig. 8 we have plotted the equation of state parameter $\omega = p/\rho$ from equations (6.4), (32) and (31), using the parameter values $\alpha = 1.58, m = 4.03$ and $n = -1.71$ from our table. We notice that $\omega(z)$ is positive early on, signifying deceleration, and then flips signature to negative at the redshift $z_{tr} = 0.89 \pm 0.25$, indicating late-time acceleration as per observations.

In summary, the behavior of the energy density and pressure in cosmology is intimately tied to the composition of the universe. Matter, radiation and dark energy each have distinct behavior, and their contributions to the energy density and pressure evolve differently with cosmic time, influencing the overall dynamics of the expansion and acceleration of the universe. Understanding these behaviors is essential for constructing cosmological models and explaining the observed features of our universe.

In the context of the dark energy concept, if $\omega > -1$, then the DE model is dubbed quintessence and if $\omega < -1$, then the model is dubbed the phantom model. In our model, the EoS parameter is positive initially and continues its evolution with negative values after a certain time. It evolves into the phantom region, crossing the Λ CDM ($\omega = -1$) divide during late times.

7. ENERGY CONDITIONS

Energy conditions in the context of modified theories of gravity, such as those beyond Einstein’s General Theory of Relativity (GR), are somewhat different from the energy conditions in standard GR. These energy conditions are used to constrain and describe the behavior of energy and matter in these alternative theories of gravity. Below are some commonly used energy conditions in modified gravity theories, along with their physical interpretations:

Null Energy Condition (NEC):

Mathematical Form: $T_{ab}k^ak^b \geq 0$ for all null vectors k^a , where T_{ab} is the energy-momentum tensor.

Physical Interpretation: In modified gravity theories, the NEC is often retained. It signifies that the energy density, as measured along null geodesics (light rays), remains non-negative. This condition ensures that light rays do not focus or converge, similar to GR.

Weak Energy Condition (WEC):

Mathematical Form: $T_{ab}v^av^b \geq 0$ for all timelike vectors v^a .

Physical Interpretation: Like in GR, the WEC implies that the energy density, as measured by an observer at rest in any reference frame, must be non-negative. This condition helps to ensure that matter has positive energy and does not violate fundamental energy principles. We also expect the WEC to be obeyed in order to achieve a transition from deceleration to acceleration.

Strong Energy Condition (SEC):

Mathematical Form: $(T_{ab} - (1/2)g_{ab}T)v^av^b \geq 0$ for all timelike vectors v^a .

Physical Interpretation: In modified gravity theories, the SEC is expected to be violated corresponding the the late-time acceleration of the universe. It implies that the gravitational effects of matter must act as a source of attractive gravity, just as in GR.

Dominant Energy Condition The dominant energy condition stipulates that, in addition to the weak energy condition holding true, for every future-pointing causal vector field (either timelike or null) v^a , the vector field $-T_b^av^b$ must be a future-pointing causal vector, i.e, mass-energy can never be observed to be flowing faster than light. However, again with dark energy, the DEC is expected to be violated corresponding the the late-time acceleration of the universe.

It is important to note that modified gravity theories often introduce additional terms and degrees of freedom into the gravitational field equations compared to GR. These additional terms can affect the interpretation and validity of the energy conditions. Also we find the energy conditions in terms of the energy density and pressure:

Trace energy condition (TEC), now abandoned
 Null energy condition (NEC): $\rho + p \geq 0$,
 Weak energy condition (WEC): $\rho \geq 0$ and $\rho + p \geq 0$,
 Strong energy condition (SEC) $\rho + 3p \geq 0$ and $\rho + p \geq 0$,
 Dominant energy condition (DEC) $\rho \geq 0$ and $-\rho \leq p \leq \rho$

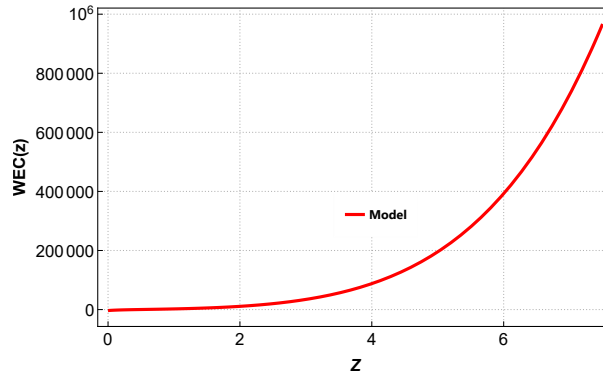


Figure 9. Figure of the *WEC*.

In Fig. 9, we have plotted the weak energy condition (WEC) against redshift z using equations (31) and (32) and the values of the parameters $\alpha = 1.58, m = 4.03$ and $n = -1.71$ as in our table. We see that the WEC is satisfied.

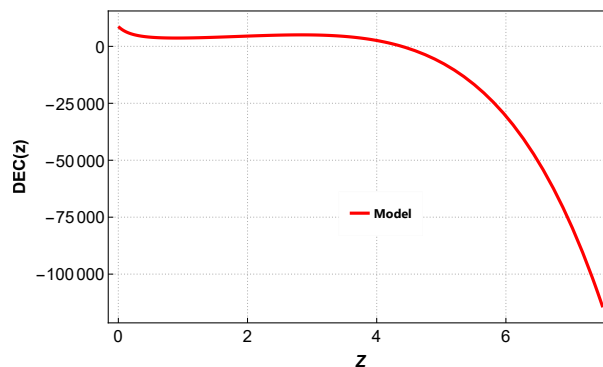


Figure 10. Figure of the *DEC*.

Fig. 10 plots the DEC against redshift using equations (31) and (32) and the values of the parameters $\alpha = 1.58, m = 4.03$ and $n = -1.71$ as in our table. It can be seen that the DEC is violated, in keeping with the requirements for a transition from deceleration to acceleration.

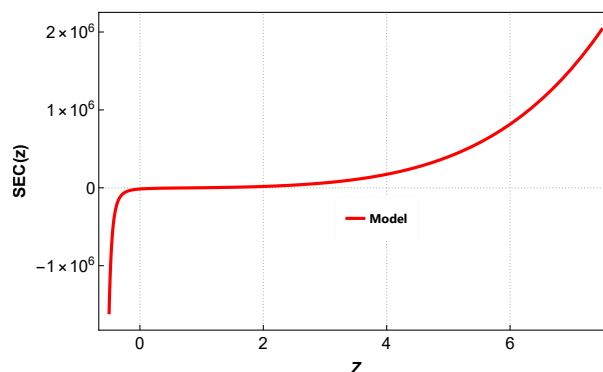


Figure 11. Figure of the *SEC*.

Fig. 11 plots the SEC against redshift using equations (31) and (32) and the values of the parameters $\alpha = 1.58, m = 4.03$ and $n = -1.71$ as in our table. It can be seen that the SEC is violated, in keeping with the requirements for a transition from deceleration to acceleration.

In summary, energy conditions in modified theories of gravity serve as a tool to understand the behavior of matter and energy in these theories. While some energy conditions may remain similar to GR, others can

be modified or relaxed, depending on the specific theory. These conditions help physicists analyze the implications of alternative gravity theories and their compatibility with observational data and fundamental physical principles. We note that in our model, the SEC and DEC are not satisfied, in keeping with a model with dark energy that has a transition from early deceleration to late-time acceleration.

8. CONCLUSION

In this work, we have studied an FLRW model in $f(\mathcal{R}, \mathcal{L}_m)$ gravity. After an introduction and background to the theory, we give a review in section 2. In section 3, we present our model. The extension presents a fresh perspective on understanding gravitational dynamics by simultaneously incorporating the geometric property of curvature and the energy distribution described by the matter Lagrangian density. Most studies involving Dark Energy in modified theories have to make some assumption on one of the parameters such as the scale factor, Hubble parameter or deceleration parameter. Here we assume a specific form for the EoS, viz., equation (19), which is not so common in the literature, and we study a solution which exhibits a transition from deceleration to acceleration. This is illustrated in Fig-3, showing that the deceleration parameter q changes sign from positive (deceleration) to negative (acceleration) at late-times.

We now make parallels with other similar works in the literature, pointing out the differences with our work. Jaybhaye et al [45] studied a model with a similar form of $f(\mathcal{R}, \mathcal{L}_m)$ as ours, but with the addition of a constant. However, their study was limited to the matter dominated universe only, i.e., $p = 0$. Hence, the energy conditions could not be discussed. Maurya [46] used a similar form for $f(\mathcal{R}, \mathcal{L}_m)$ as [45], but added a constant coefficient to the \mathcal{L}_m^α term. There was no discussion of the energy density, pressure and the energy conditions. The other paper that bears close resemblance to ours is that of Myrzakulov et al [47]. Those authors used the same form for $f(\mathcal{R}, \mathcal{L}_m)$, but they chose a different form for the EoS parameter. According to the deceleration parameter, there is a transition from deceleration to acceleration, but the pressure and EoS parameter remain negative throughout, indicating acceleration only. There is also no discussion of the energy conditions. In our work, the energy density is non-negative throughout. On the other hand, the deceleration parameter, pressure and EoS parameter show signature flips as required for a transition from deceleration to acceleration. We have provided a complete analysis of the energy conditions, showing that the WEC is satisfied, but both the DEC and SEC are violated. Again, this is in keeping with the change from deceleration to acceleration.

In section 4, we subjected the model to observational tests, and obtained the best fit values of the model parameters, viz., $H_0 = 69 \pm 0.012$, $\alpha = 1.58_{-0.35}^{+0.29}$, $m = 4.03_{-0.59}^{+0.29}$, and $n = -1.71_{-0.11}^{+0.11}$. In addition, we discussed the various cosmographic parameters in section 5 and illustrated by means of graphs. The deceleration parameter q , and the diagnostic pair (r, s) have been discussed in section 5, and illustrated by means of figures. Then, in section 6, the physical parameters ρ and p and the energy conditions are analysed. The energy density ρ is positive throughout, and the pressure p has a signature flip from positive (deceleration) to negative (acceleration). We have studied the energy conditions and showed that they are also compatible with the transition from deceleration to acceleration, i.e., the WEC is satisfied, but the DEC and SEC are not satisfied, and exhibit a signature flip associated with late-time acceleration.

In conclusion, we have studied an FLRW model in $f(\mathcal{R}, \mathcal{L}_m)$ gravity by utilising a form for the EoS. The model is compatible with observations, and is worthy of further study. In this work, we have chosen probably the most simple form for $f(\mathcal{R}, \mathcal{L}_m)$, i.e., $f(\mathcal{R}, \mathcal{L}_m) = R/2 + \mathcal{L}_m^\alpha$. However, it allows us to study the departure from general relativity, and what differences arise. Future prospects include extending to more complicated forms of $f(\mathcal{R}, \mathcal{L}_m)$, e.g., other functions of $f(R)$ since $f(R)$ theories have been well-studied in the literature [48]. In addition, one can consider other forms of \mathcal{L}_m^α .

ORCID

 **Bhupendra Kumar Shukla**, <https://orcid.org/0000-0002-4318-2356>;  **R.K. Tiwari**, <https://orcid.org/0009-0002-6931-3067>;  **D. Sofuoğlu**, <https://orcid.org/0000-0002-8842-7302>;  **A. Bee-sham**, <https://orcid.org/0000-0001-5350-6396>

REFERENCES

- [1] A.G. Riess, et al., *Astron. J.* **116**, 1009 (1998). <https://doi.org/10.1086/300499>
- [2] S. Perlmutter, et al., *Astrophys. J.* **517**, 565 (1999). <https://doi.org/10.1086/307221>
- [3] C.L. Bennett, et al., *Astrophys. J. Suppl.* **148**, 119-134 (2003). <https://doi.org/10.1086/377253>
- [4] R.R. Caldwell, and M. Doran, *Phys. Rev. D*, **69**, 103517 (2004). <https://doi.org/10.1103/PhysRevD.69.103517>
- [5] D.N. Spergel, et al., [WMAP Collaboration], *Astrophys. J. Suppl.* **148**, 175 (2003). <https://doi.org/10.1086/377226>
- [6] D.J. Eisenstein, et al., *Astrophys. J.* **633**, 560 (2005). <https://doi.org/10.1086/466512>

- [7] W.J. Percival, et al., *Mon. Not. R. Astron. Soc.* **401**, 2148 (2010). <https://doi.org/10.1111/j.1365-2966.2009.15812.x>
- [8] T. Koivisto, D.F. Mota, *Phys. Rev. D*, **73**, 083502 (2006). <https://doi.org/10.1103/PhysRevD.73.083502>
- [9] S.F. Daniel, *Phys. Rev. D*, **77**, 103513 (2008). <https://doi.org/10.1103/PhysRevD.77.103513>
- [10] S. Weinberg, *Rev. Mod. Phys.* **61**, 1 (1989). <https://doi.org/10.1103/RevModPhys.61.1>
- [11] E.J. Copeland et al., *Int. J. Mod. Phys. D*, **15**, 1753 (2006). <https://doi.org/10.1142/S021827180600942X>
- [12] A.A. Starobinsky, *Gravit. Cosmol.* **6**, 157 (2000). https://doi.org/10.1142/9789812793324_0008
- [13] R.R. Caldwell, *Phys. Lett. B*, **545**, 23 (2002). [https://doi.org/10.1016/S0370-2693\(02\)02589-3](https://doi.org/10.1016/S0370-2693(02)02589-3)
- [14] R.R. Caldwell, M. Kamionkowski, and N.N. Weinberg, *Phys. Rev. Lett.* **91**, 071301 (2003). <https://doi.org/10.1103/PhysRevLett.91.071301>
- [15] S. Capozziello, *Int. J. Mod. Phys. D*, **11**, 483 (2002). <https://doi.org/10.1142/S0218271802002025>
- [16] T. Harko, and F.S.N. Lobo, *Eur. Phys. J. C*, **70**, 373 (2010). <https://doi.org/10.1140/epjc/s10052-010-1467-3>
- [17] T. Harko, *Phys. Lett. B*, **669**, 376 (2008). <https://doi.org/10.1016/j.physletb.2008.10.007>
- [18] T. Harko, *Phys. Rev. D*, **81**, 084050 (2010). <https://doi.org/10.1103/PhysRevD.81.084050>
- [19] T. Harko, *Phys. Rev. D*, **81**, 044021 (2010). <https://doi.org/10.1103/PhysRevD.81.044021>
- [20] S. Nesseris, *Phys. Rev. D*, **79**, 044015 (2009). <https://doi.org/10.1103/PhysRevD.79.044015>
- [21] V. Faraoni, *Phys. Rev. D*, **76**, 127501 (2007). <https://doi.org/10.1103/PhysRevD.76.127501>
- [22] V. Faraoni, *Phys. Rev. D*, **80**, 124040 (2009). <https://doi.org/10.1103/PhysRevD.80.124040>
- [23] V. Faraoni, *Cosmology in Scalar-Tensor Gravity*, (Kluwer Academic, Dordrecht, 2004).
- [24] O. Bertolami, J. Paramos, and S. Turyshev, (2006). <https://doi.org/10.48550/arXiv.gr-qc/0602016>
- [25] J. Wang, and K. Liao, *Class. Quantum Grav.* **29**, 215016 (2012). <https://doi.org/10.1088/0264-9381/29/21/215016>
- [26] B.S. Goncalves, P.H.R.S. Moraes, and B. Mishra (2023). <https://doi.org/10.48550/arXiv.2101.05918>
- [27] R. Solanki, B. Patel, L.V. Jaybhaye, and P.K. Sahoo, *Commun. Theor. Phys.* **75**, 075401 (2023). <https://doi.org/10.1088/1572-9494/acd4aa>
- [28] L.V. Jaybhaye, R. Solanki, S. Mandal, and P.K. Sahoo, *Universe*, **9**, 163 (2023). <https://doi.org/10.3390/universe9040163>
- [29] M. Zeyauddin, A. Dixit, and A. Pradhan, *Int. J. Geom. M. Modern Phys.* (2023). <https://doi.org/10.1142/S0219887824500385>
- [30] N. Myrzakulov, M. Koussour, A.H.A. Alnadhief, A. Abebe, *Eur. Phys. J. P.* **138**, 852 (2023). <https://doi.org/10.1140/epjp/s13360-023-04483-3>
- [31] D.C. Maurya, *Grav. Cosm.* **29**, 315 (2023). <https://doi.org/10.1134/S020228932303012X>
- [32] R. Solanki, et al. *Commun. Theor. Phys.* **75**, 075401 (2023). <https://doi.org/10.1088/1572-9494/acd4aa>
- [33] J.K. Singh, et al., *New Astr.* **104**, 102070 (2023). <https://doi.org/10.1016/j.newast.2023.102070>
- [34] L.V. Jaybhaye et al., *Phys. Dark Univ.* **40**, 101223 (2023). <https://doi.org/10.1016/j.dark.2023.101223>
- [35] J.C. Fabris et al., *Eur. Phys. J. Plus*, **138**, 232 (2023). <https://doi.org/10.1140/epjp/s13360-023-03845-1>
- [36] A. Pradhan et al., *Int. J. Geom. M. Mod. Phys.* **20**, 1230105 (2023).
- [37] D.C. Maurya, *New Astr.* **100**, 101974 (2023). <https://doi.org/10.1016/j.newast.2022.101974>
- [38] G.A. Carvalho, et al., *Eur. Phys. J. C*, **82**, 1096 (2022). <https://doi.org/10.1140/epjc/s10052-022-11058-6>
- [39] R.V. Labato, G.A. Carvalho, and C.A. Bertulani, *Eur. Phys. J. C*, **81**, 1013 (2021). <https://doi.org/10.1140/epjc/s10052-021-09785-3>
- [40] T. Harko and S. Shahidi, *Eur. Phys. J. C*, **82**, 1003 (2022). <https://doi.org/10.1140/epjc/s10052-022-10891-z>
- [41] T. Harko and M.J. Lake, *Eur. Phys. J. C*, **75**, 60 (2015). <https://doi.org/10.1140/epjc/s10052-015-3287-y>
- [42] T. Harko and F.S.N. Lobo, *Galaxies*, **2014**(2), 410-465 (2014). <https://doi.org/10.3390/galaxies2030410>
- [43] M. Chevallier and D. Polarski, *Int. J. Mod. Phys. D*, **10**, 213 (2001). <https://doi.org/10.1142/S0218271801000822>
- [44] E.V. Linder, *Phys. Rev. Lett.* **90**, 091301 (2003). <https://doi.org/10.1103/PhysRevLett.90.091301>
- [45] Jaybhaye, et al., *Phys. Lett. B* **831**, 137148 (2022). <https://doi.org/10.1016/j.physletb.2022.137148>
- [46] D.C. Maurya, *Grav. Cosm.* **29**, 315-325 (2023) <https://doi.org/10.1134/S020228932303012X>
- [47] N. Myrzakulov, et al., *Eur. Phys. J. P.* (2023). <https://doi.org/10.1140/epjp/s13360-023-04483-3>
- [48] A. De Felice and S. Tsujikawa, *Living Rev. Rel.* **13**, 3 (2010). <https://doi.org/10.12942/lrr-2010-3>

ВСЕСВІТ FLRW У ГРАВІТАЦІЇ $f(\mathcal{R}, \mathcal{L}_m)$ З РІВНЯННЯМ ПАРАМЕТРА СТАНУБхупендра Кумар Шукла^a, Р.К. Тіварі^b, Д. Софуоглу^c, А. Бішем^{d,e,f}^a Департамент математики, Держ. Коледж Bandri Sagar, 470442 (М.Р.) Індія^b Департамент математики, Держ. Model Science College Rewa 486 001 (М.Р.) Індія^c Кафедра фізики Стамбульського університету Везнеджилер 34134, Фатіх, Стамбул, Туреччина^d Департамент математичних наук, Університет Зулуленду,

P Bag X1001, Ква-Dlangezwa 3886, Південна Африка

^e Факультет природничих наук, Технологічний університет Мангосуту,

PO Box 12363, Джейкобс, Південна Африка

^f Національний інститут теоретичних і обчислювальних наук, Південна Африка

Наявні дані спостережень щодо сучасних космологічних характеристик свідчать про те, що Всесвіт значною мірою є ізотропним і однорідним у великому масштабі. У цьому дослідженні наша мета полягає в аналізі просторового часу Фрідмана-Леметра-Робертсона-Уокера (FLRW) за допомогою ідеального розподілу рідини. Ми спеціально досліджуємо структуру $f(\mathcal{R}, \mathcal{L}_m)$ гравітації в межах певних обмежень. Щоб досягти цього, ми зосереджуємося на конкретній нелінійній моделі $f(\mathcal{R}, \mathcal{L}_m)$, представленій як $f(\mathcal{R}, \mathcal{L}_m) = \frac{\mathcal{R}}{2} + \mathcal{L}_m^\alpha$. Рівняння поля розв'язуються за допомогою рівняння параметра стану виду параметризації Шевальє-Полярського-Ліндера (CPL). Дослідження параметрів уповільнення виявляє прискорення Всесвіту в пізній час. Перехідне червоне зміщення виявлено $z_{tr} = 0,89 \pm 0,25$. Також ми обговорили фізичні та геометричні властивості моделі.

Ключові слова: $f(\mathcal{R}, \mathcal{L}_m)$ гравітація; темна енергія; прискорення Всесвіту; рівняння параметра стану